Materials Science and Technology

ISSN: 0267-0836 (Print) 1743-2847 (Online) Journal homepage: http://www.tandfonline.com/loi/ymst20

# Artificial neural network modelling to predict hot deformation behaviour of zinc–aluminium alloy

Y Liu, H Y Li, H F Jiang & X J Su

**To cite this article:** Y Liu, H Y Li, H F Jiang & X J Su (2013) Artificial neural network modelling to predict hot deformation behaviour of zinc–aluminium alloy, Materials Science and Technology, 29:2, 184-189, DOI: 10.1179/1743284712Y.0000000127

**To link to this article:** https://doi.org/10.1179/1743284712Y.0000000127

Published online: 12 Nov 2013.

Submit your article to this journal

Article views: 51

View related articles

Citing articles: 7 View citing articles

Full Terms & Conditions of access and use can be found at
http://www.tandfonline.com/action/journalInformation?journalCode=ymst20

# Artificial neural network modelling to predict hot deformation behaviour of zinc–aluminium alloy

**Y. Liu, H. Y. Li*, H. F. Jiang and X. J. Su**

Isothermal hot compression of ZA27 alloy was conducted on a Gleeble-1500 thermomechanical simulator in the temperature range of 473–523 K with strain rates of 0·01–5 $s^{-1}$ and height reduction of 60%. Based on the experimental results, an artificial neural network (ANN) model with a backpropagation learning algorithm was developed for the description and prediction of the hot deformation behaviour. The inputs of the model are temperature, strain rate and strain. The output of the model is the flow stress. Then, a comparative evaluation of the trained ANN model and the constitutive equations was carried out. It was found that the trained ANN model was more efficient and accurate in predicting the hot deformation behaviour of ZA27 alloy.

**Keywords:** ZA27 alloy, Hot deformation behaviour, Artificial neural network, Constitutive equation, Flow stress

## Introduction

Zinc–aluminium (ZA) alloys were first developed based on the ZAMAK alloys in North America in the 1970s.[1] The aluminium content was selected as about 8, 12, 22 and 27 wt-%, and the copper content was up to 3 wt-%. They were named after their aluminium content as ZA8, ZA12, ZA22 and ZA27.[2,3] Among the family of ZA alloys, ZA27 alloy exhibits favourable physical and mechanical properties combined with high tensile strength and wear resistance properties, making it an attractive alternative to their conventional counterparts like aluminium casting alloys, copper based alloys and cast iron in various engineering applications.[4,5]

The hot deformation behaviour of materials is quite important for the optimisation of the thermomechanical process parameters as it directly affects the microstructure evolution of the materials and the mechanical properties of the formed product.[6] In order to describe the hot deformation behaviours of materials and optimise the thermomechanical process parameters, many research groups have made use of the regression methods to develop constitutive equations over the past few years.[7,8] However, development of such constitutive equations is always time consuming. Moreover, the response of the deformation behaviours of materials under elevated temperatures and strain rates and the effects of many factors on the flow stress are often non-linear, which reduce the accuracy of prediction.

The artificial neural networks (ANNs) can be a good candidate to solve the problems that are the most difficult to solve by the regression methods. The ANN model can learn from training data and recognise patterns in a series of input and output values without any prior assumptions about their nature and interrelations.[9] Up to now, a comprehensive study on hot deformation behaviour using ANN models has been carried out on alloy steel,[10–12] aluminium alloy,[13] magnesium alloy,[14] titanium alloy,[15] nickel alloy[16] and metal matrix composites.[17] However, little studies on ANN models to explore the hot deformation behaviour of ZA alloy are recordable in the scientific literature.

In the present study, a three-layer feed forward ANN with a backpropagation learning algorithm was established to explore and predict the flow behaviour of ZA27 alloy. In addition, constitutive equations were developed to predict the flow stress of ZA27 alloy. Furthermore, a comparative evaluation of the constitutive equations and the trained ANN model was carried out.

## Experimental

The experimental ZA27 alloys were prepared from commercially pure Al (99·99 wt-%), Zn (99·99 wt-%), Mg (99·99 wt-%) and Al–Cu master alloy (37·41 wt-%Cu), which were charged in a graphite crucible and then melted in a resistance furnace at 700°C. After thorough stirring, the melt was cast into a preheated mild steel mould at 600°C. The cast ingot was homogenised at 360°C for 12 h and then furnace cooled to room temperature. The composition of the investigated alloys in the as cast state are given in Table 1, as measured by inductively coupled plasma atomic emission spectroscopy.

The specimens for isothermal compression tests were machined into cylinder with 15 mm in height and 10 mm in diameter. In order to minimise the friction between the specimens and die during hot compression, flat bottomed grooves with a depth of 0·1 mm were

School of Materials Science and Engineering, Central South University, Changsha 410083, China

*Corresponding author, email lhying@mail.csu.edu.cn

© 2013 Institute of Materials, Minerals and Mining
Published by Maney on behalf of the Institute
Received 3 August 2012; accepted 15 September 2012
DOI 10.1179/1743284712Y.0000000127

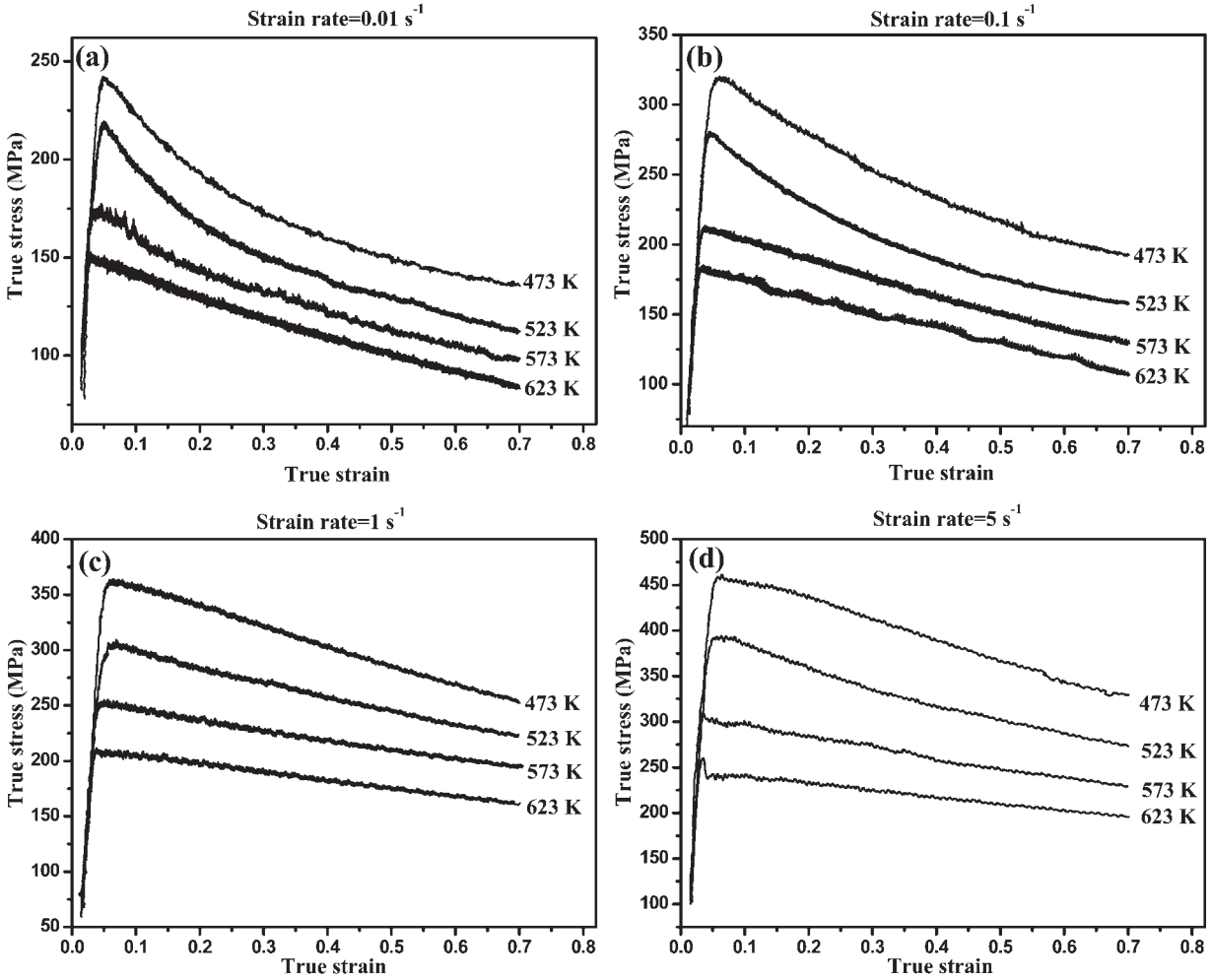


**1 True stress–true strain curves of ZA27 alloy at various temperatures with strain rate of *a* 0·01 $s^{-1}$, *b* 0·1 $s^{-1}$, *c* 1 $s^{-1}$ and *d* 5 $s^{-1}$**

machined in the undersurface to entrap the lubricant of graphite mixed with machine oil. The hot compression tests were conducted on a Gleeble 1500 thermal simulator machine at 473, 523, 573 and 623 K with strain rates of 0·01, 0·1, 1 and 5 $s^{-1}$. The reduction in height is 60% at the end of the compression tests. The deformation temperature is measured by thermocouples that are welded to the centre region of the specimen surface. Before the hot compression, each specimen was heated to the deformation temperature at a rate of 10 K $s^{-1}$ and held for 3 min to ensure the uniform temperature of the specimens. All the tests were carried out under isothermal conditions with temperature being maintained within $\pm 2$ K. The specimens were immediately quenched in water after deformation to retain the microstructures at elevated temperature.

## Results and discussion

### True stress–true strain curves

The true stress–strain curves obtained from the hot compression tests of ZA27 alloy are shown in Fig. 1. It can be seen that all the curves exhibit the typical shape for dynamic recrystallisation, i.e. strain hardening to a peak stress followed by flow softening. At the lower strain rates (0·01 and 0·1 $s^{-1}$) and lower deformation temperature (473 and 523 K), the curves undergo a single peak stress followed by a rapid decline, and the decline rate decreases as the true strain increases. At the higher strain rates of 1 and 5 $s^{-1}$, the flow stress decreases with the increase in strain, and the decline rate decreases as the temperature rises.

**Table 1 Composition of experimental ZA27 alloy (wt-%)**

| Al | Cu | Mg | Zn |
|---|---|---|---|
| 27·10 | 2·09 | 0·01 | Bal. |

Figure 2 shows the effect of deformation temperatures and strain rates on the flow stress at a true strain of 0·4. It can be found that the flow stress of ZA27 alloy is sensitive to the effect of deformation temperatures and strain rates. The flow stress generally decreases with the increase in deformation temperature at a given strain rate and increases with the increase in strain rates at a given temperature. This is due to the fact that higher temperatures and lower strain rates can offer higher mobility at boundaries for the nucleation and growth of dynamically recrystallised grains, and longer time for energy accumulation and dislocation annihilation.

### Modelling with ANN

A three-layer feed forward back propagation ANN (as shown in Fig. 3) was employed to predict the flow behaviour and model the constitutive relationship of ZA27 alloy. The input layer is used to receive data from

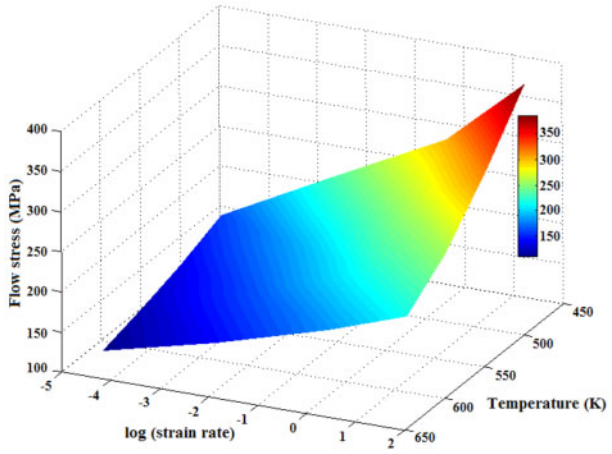


**2 Effect of temperature and strain rates on flow stress at strain of 0·4**

outside, and the output layer sends the information out, while the hidden layer that contains a systematically determined number of processing elements is to provide the necessary complexity for non-linear problems. In the present work, the strain $\varepsilon$, strain rate $\dot{\varepsilon}$ and deformation temperature $T$ were chosen as the inputs, and the flow stress $\sigma$ was chosen as the output of the model.

In order to obtain a usable form for the network to read, both input and output variables should be normalised within the range from 0 to 1 before the training of the network. The following equation is used widely for unification

$$X' = \frac{X - 0{\cdot}95X_{\min}}{1{\cdot}05X_{\max} - 0{\cdot}95X_{\min}} \tag{1}$$

where $X$ is the original data, $X'$ is the unified data of the corresponding $X$, and $X_{\min}$ and $X_{\max}$ are the minimum and maximum value of $X$ respectively. This equation was used in the present paper to unify data $T$, $\varepsilon$ and $\sigma$. However, because $\dot{\varepsilon}$ changed sharply and after unification the minimum value of $\dot{\varepsilon}$ was too small for the ANN to learn, the following equation is adopted to unify the value of $\dot{\varepsilon}$

$$\dot{\varepsilon}' = \frac{(3+\lg\dot{\varepsilon}) - 0{\cdot}95(3+\lg\dot{\varepsilon}_{\min})}{1{\cdot}05(3+\lg\dot{\varepsilon}_{\max}) - 0{\cdot}95(3+\lg\dot{\varepsilon}_{\min})} \tag{2}$$

in which a constant 3 is added in order to make the unified data be positive.

In the present ANN model, 592 data sets selected from the true stress–strain curves were divided into two sets: a training dataset and a test dataset. During establishing the ANN model, 384 data sets were used to train the network model, and the other 208 data sets at

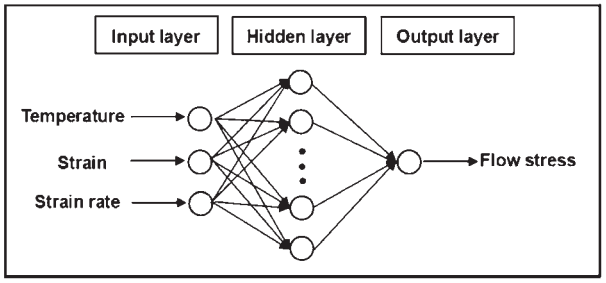


**3 Architecture of BP ANN in present work**

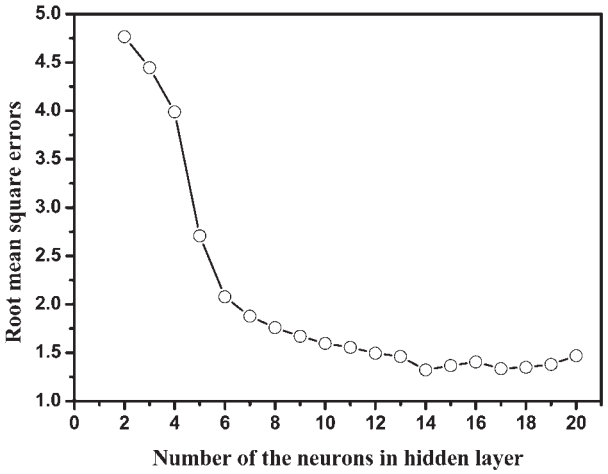


**4 Performance of network at different hidden neurons**

true strain between 0·1 and 0·7 with interval of 0·05 were applied to test the performance of the ANN model. In order to determine the appropriate number of neurons in the hidden layer, the trial and error procedure was started with two neurons in the hidden layer and further carried out with more neurons. Figure 4 showed the influence of the number of neurons in hidden layer on the network performance. It was found that a network with one hidden layer consisting of 14 hidden neurons gave a minimum average root mean square error (RMSE) and therefore considered as the optimal structure for the prediction of flow stress of ZA27 alloy. The ANN achieved a stable state after 12 000 cycles of training.

## Modelling constitutive relationship

The combined effects of strain rate and temperature on deformation behaviour could be represented by the Zener–Hollomon parameter $Z$ in an exponent type equation,[18] as shown in equation (3). Furthermore, the relationships between flow stress, strain rate and deformation temperature can be shown in equations (4)–(6)[19]

$$Z = \dot{\varepsilon}\exp\left(\frac{Q}{RT}\right) \tag{3}$$

$$\dot{\varepsilon} = A_1\sigma^{n_1}\exp\left(-\frac{Q}{RT}\right) \tag{4}$$

$$\dot{\varepsilon} = A_2\exp(\beta\sigma)\exp\left(-\frac{Q}{RT}\right) \tag{5}$$

$$\dot{\varepsilon} = A[\sinh(\alpha\sigma)]^n\exp\left(-\frac{Q}{RT}\right) \tag{6}$$

where $\dot{\varepsilon}$ is the strain rate ($s^{-1}$), $Q$ is the activation energy of hot deformation (kJ $mol^{-1}$), $R$ is the universal gas constant (8·314 J $mol^{-1}$ $K^{-1}$), $T$ is the absolute temperature (K) and $\sigma$ is the flow stress (MPa). $A_1$, $A_2$, $A$, $n_1$, $n$, $\alpha$ and $\beta$ are the material constants independent of the temperature for a particular strain, $\alpha = \beta/n_1$. The power law, equation (4), and the exponential law, equation (5), are suitable for the low stress ($\alpha\sigma < 0{\cdot}8$) and the high stress ($\alpha\sigma > 1{\cdot}2$) respectively. However, the hyperbolic sine law, equation (6), can be used over a wide range of deformation conditions.

In the present study, flow stress, strain rate and deformation temperature data for the true strain

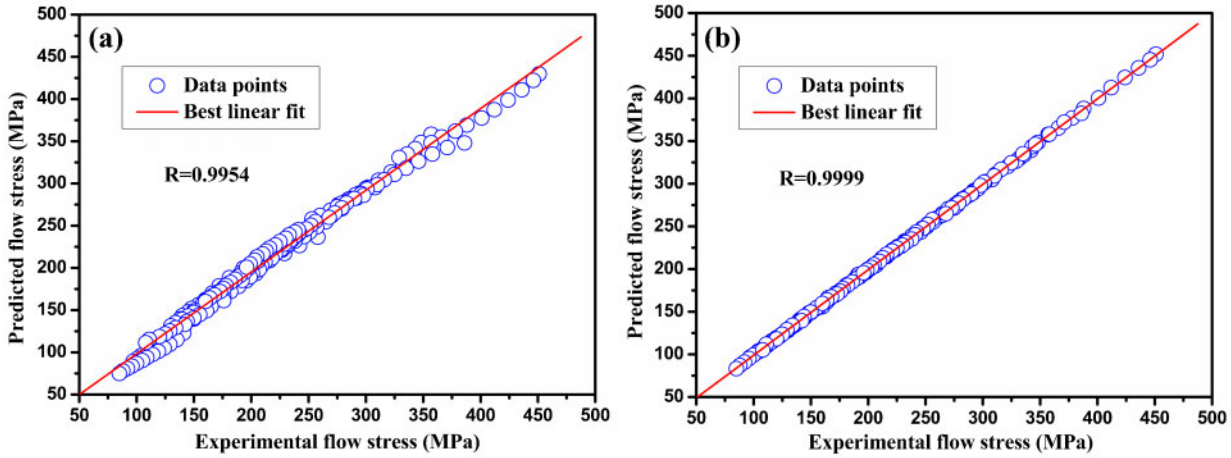


*a* by constitutive equations; *b* by ANN model

**5 Correlation between experimental and predicted flow stress**

between 0·1 and 0·7 with interval of 0·05 were adopted to construct constitutive equations respectively. Based on equations (3)–(6), the parameters $A_1$, $A_2$, $A$, $\beta$, $\alpha$, $n$ and $Q$ of ZA27 alloy can be calculated by the regression method, and the constant ($A$, $\alpha$, $n$ and $Q$) values of the constitutive equations for each true strain are listed in Table 2.

After the material constants are evaluated, the flow stress at a particular strain can be predicted. Then, the flow stress can be written as a function of the Zener–Hollomon parameter, considering the definition of the hyperbolic law, as shown in equation (7)

$$\sigma = \frac{1}{\alpha}\ln\left\{\left(\frac{Z}{A}\right)^{1/n} + \left[\left(\frac{Z}{A}\right)^{2/n} + 1\right]^{1/2}\right\} \tag{7}$$

## Comparison between constitutive equation and ANN model

The predictability of the trained ANN model and the constitutive equation is verified via employing standard statistical parameters such as correlation coefficient $R$, average absolute relative error (AARE), average RMSE and relative error. They are expressed as

**Table 2 Constant values of constitutive equation for each true strain**

| | Constants values | | | |
|---|---|---|---|---|
| Strain | $A/s^{-1}$ | $\alpha/MPa^{-1}$ | $n$ | $Q/kJ\ mol^{-1}$ |
| 0·1 | $1{\cdot}470\times10^{11}$ | $4{\cdot}203\times10^{-3}$ | 7·532 | 95·513 |
| 0·15 | $1{\cdot}961\times10^{10}$ | $4{\cdot}373\times10^{-3}$ | 7·046 | 88·818 |
| 0·2 | $4{\cdot}071\times10^{9}$ | $4{\cdot}574\times10^{-3}$ | 6·699 | 83·285 |
| 0·25 | $8{\cdot}104\times10^{8}$ | $4{\cdot}474\times10^{-3}$ | 6·446 | 77·312 |
| 0·3 | $2{\cdot}223\times10^{8}$ | $4{\cdot}873\times10^{-3}$ | 6·248 | 73·322 |
| 0·35 | $1{\cdot}044\times10^{8}$ | $4{\cdot}992\times10^{-3}$ | 6·103 | 70·613 |
| 0·4 | $5{\cdot}357\times10^{7}$ | $5{\cdot}182\times10^{-3}$ | 5·999 | 68·427 |
| 0·45 | $2{\cdot}548\times10^{7}$ | $5{\cdot}314\times10^{-3}$ | 5·787 | 66·160 |
| 0·5 | $1{\cdot}284\times10^{7}$ | $5{\cdot}454\times10^{-3}$ | 5·633 | 63·277 |
| 0·55 | $8{\cdot}870\times10^{6}$ | $5{\cdot}583\times10^{-3}$ | 5·554 | 61·951 |
| 0·6 | $5{\cdot}386\times10^{6}$ | $5{\cdot}731\times10^{-3}$ | 5·442 | 60·169 |
| 0·65 | $4{\cdot}997\times10^{6}$ | $5{\cdot}856\times10^{-3}$ | 5·328 | 60·246 |
| 0·7 | $5{\cdot}234\times10^{6}$ | $5{\cdot}982\times10^{-3}$ | 5·264 | 59·738 |

$$R = \frac{\sum_{i=1}^{N}(E_i-\bar{E})(P_i-\bar{P})}{\left[\sum_{i=1}^{N}(E_i-\bar{E})^2(P_i-\bar{P})^2\right]^{1/2}} \tag{8}$$

$$\text{AARE} = \frac{1}{N}\sum_{i=1}^{N}\left|\frac{E_i-P_i}{E_i}\right| \times 100\% \tag{9}$$

$$\text{RMSE} = \left[\frac{1}{N}\sum_{i=1}^{N}(E_i-P_i)^2\right]^{1/2} \tag{10}$$

$$\text{Relative error} = \left(\frac{E_i-P_i}{E_i}\right) \times 100\% \tag{11}$$

where $E_i$ and $P_i$ are the experimental and predicted value respectively; $\bar{E}$ and $\bar{P}$ are the mean values of $E_i$ and $P_i$ respectively; and $N$ is the total number of data employed in the investigation. The correlation coefficient $R$ is a commonly used statistical parameter, which provides information on the strength of linear relationship between the experimental and the predicted values.[20] The AARE and RMSE are calculated through a term by term comparison of the relative error and therefore are unbiased statistics for verifying the predictability of a model or equation.[21]

Figure 5 shows the plot of experimental values and predicted values by the ANN model as well as calculated values by the constitutive equations respectively. It is clearly seen that most of the data points lie exactly close to the line, and the correlation coefficient $R$ for the ANN model and the constitutive equations is 0·9999 and 0·9954 respectively. This means that a better correlation between the predicted and the experimental data has been achieved by the ANN model. The AAREs are 0·57 and 1·89% corresponding to the ANN model and the constitutive equations. Additionally, the average RMSEs of the ANN model and the constitutive equations are obtained as 1·32 and 8·03 MPa respectively. These results indicate that the accuracy of the predicted flow stress based on the ANN model is higher than that calculated by the constitutive equations.

The statistical analysis of the relative error is represented graphically as a typical number versus relative error plot, as shown in Fig. 6. It can be obtained that the

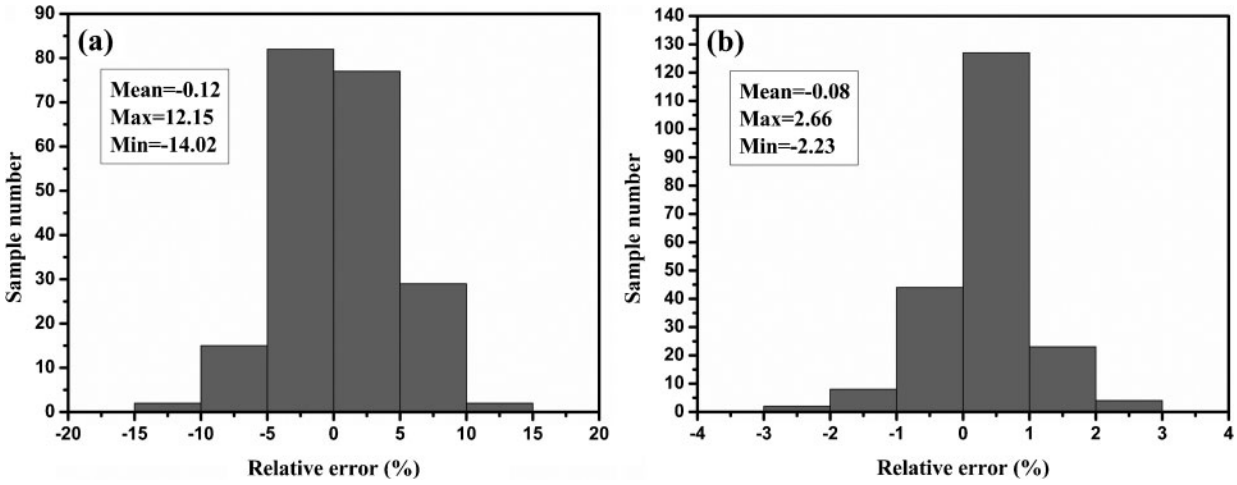


*a* by constitutive equations; *b* by ANN model

**6 Statistical analysis of relative error**

relative error based on the ANN model varies from −2·23 to 2·66%, whereas it is in the range of −14·02 to 12·15% for the constitutive equations. For more than 95% test data sets, the relative error of ANN model was shown within ±2%, while the relative error of the constitutive equations is much bigger. Therefore, the data were fitted better in the ANN model compared to the constitutive equations.

Figure 7 shows the comparison between the experimental and predicted flow stress of ZA27 alloy using the constitutive equations as well as the ANN model. It could be observed that the predicted flow stress values based on the ANN model are in a good agreement with the experimental values throughout the entire temperature and strain rate range, revealing the higher accuracy of the ANN model. Moreover, there is a deviation

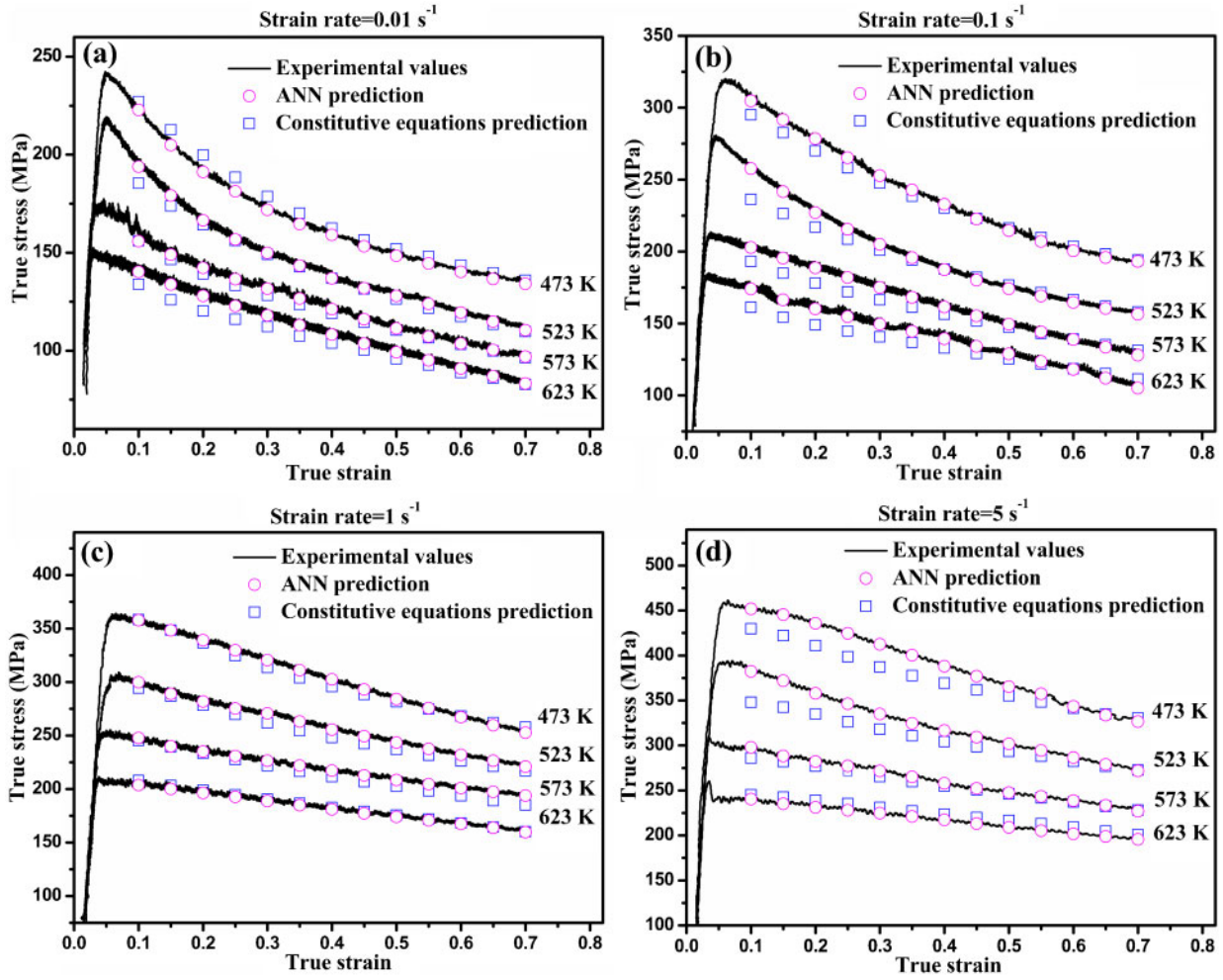


**7 Comparison of predicted with experimental flow stress of ZA27 alloy with strain rates of *a* 0·01 $s^{-1}$, *b* 0·1 $s^{-1}$, *c* 1 $s^{-1}$ and *d* 5 $s^{-1}$**

between experimental values and the predicted flow stress from the constitutive equations under some deformation condition, for instance, at 473 and 523 K in 5 $s^{-1}$, which indicates that the constitutive equations could be used to do a rough estimate.

The results obtained above obviously indicate that the well trained ANN model showed better performance and could be more accurate and effective in predicting the hot deformation behaviour of ZA27 alloy than constitutive equations. Once the computer model is available, the complicated constitutive relationship can be elaborated.

## Conclusions

The hot deformation behaviour of ZA27 alloy has been investigated by means of hot compression tests over a practical range of temperatures (473–623 K) and strain rates (0·01–5 $s^{-1}$). Based on the present study, the following conclusions can be drawn:

1. It is found that the flow stress of ZA27 alloy increases with increasing strain rate and the decrease in deformation temperature.

2. The ANN could be a powerful predicted tool to predict the flow stress without the need to evaluate a large number of constants associated with constitutive models.

3. A comparative evaluation of the trained ANN model and the constitutive equations was carried out. It is obtained that the absolute values of maximum relative error from the ANN model and the constitutive equations are 2·66 and 14·02% respectively. The AAREs are 0·57 and 1·89% corresponding to the ANN model and the constitutive equations, which indicate that the well trained ANN model can provide accurate results and has a better prediction capability than the constitutive equations.

## Acknowledgement

The authors are grateful to the Nonferrous Metals Science Foundation of HNG-CSU for the financial support (project no. Z2011-01-002).

## References

1. Y. H. Zhu: *Mater. Trans.*, 2004, **45**, 3083–3097.
2. A. Türk, M. Durman and E. S. Kayali: *J. Mater. Sci.*, 2007, **42**, 8298–8305.
3. Y. H. Zhu, S. To, X. M. Liu and G. L. Hu: *Metall. Mater. Trans. A*, 2011, **42A**, 1933–1940.
4. T. J. Chen, Y. Hao and Y. D. Li: *Mater. Des.*, 2007, **28**, 1279–1287.
5. Y. H. Zhu, S. To, W. B. Lee, S. J. Zhang and C. F. Cheung: *Scr. Mater.*, 2010, **62**, 101–104.
6. Y. C. Lin, M. S. Chen and J. Zhong: *Mater. Lett.*, 2008, **62**, 2132–2135.
7. J. Cai, F. G. Li, T. Y. Liu, B. Chen and M. He: *Mater. Des.*, 2011, **32**, 1144–1151.
8. H. Y. Li, Y. Liu, X. C. Lu and X. J. Su: *J. Mater. Sci.*, 2012, **47**, 5411–5418.
9. P. A. Lucon and R. P. Donovan: *Composite B*, 2007, **38B**, 817–823.
10. Y. C. Lin, G. Liu, M. S. Chen and J. Zhong: *J. Mater. Process. Technol.*, 2009, **209**, 4611–4616.
11. M. S. Ozerdem and S. Kolukisa: *J. Mater. Process. Technol.*, 2008, **199**, 437–439.
12. D. Samantaray, S. Mandal, A. K. Bhaduri, S. Venugopal and P. V. Sivaprasad: *Mater. Sci. Eng. A*, 2011, **A528**, 1937–1943.
13. Z. L. Lu, Q. L. Pan, X. Y. Liu, Q. J. Qin, Y. B. He and S. F. Cao: *Mech. Res. Commun.*, 2011, **38**, 192–197.
14. O. Sabokpa, A. Zarei-Hanzaki, H. R. Abedi and N. Haghdadi: *Mater. Des.*, 2012, **39**, 390–396.
15. Y. Sun, W. D. Zeng, Y. Q. Zhao, Y. L. Qi, X. Ma and Y. F. Han: *Comput. Mater. Sci.*, 2010, **48**, 686–691.
16. I. S. Jalham: *Compos. Sci. Technol.*, 2003, **63**, 63–67.
17. P. F. Bariani, S. Bruschi and T. Dal Negro: *J. Mater. Process. Technol.*, 2004, **152**, 395–400.
18. C. Zener and J. H. Hollomon: *J. Appl. Phys.*, 1944, **15**, 22–32.
19. C. M. Sellars and W. J. McTegart: *Acta Metall.*, 1966, **14**, 1136–1138.
20. M. P. Phaniraj and A. K. Lahiri: *J. Mater. Process. Technol.*, 2003, **141**, 219–227.
21. S. Srinivasulu and A. Jain: *Appl. Soft Comput.*, 2006, **6**, 295–306.